



IGFBP5 promotes EndoMT and renal fibrosis through H3K18 lactylation in diabetic nephropathy

Xiaofang Hu¹ · Wei Chen¹ · Ming Yang² · Mengwei Li¹ · Xiangyi Li³ · Shaxi Ouyang³

Received: 23 December 2024 / Revised: 25 March 2025 / Accepted: 16 April 2025
 © The Author(s) 2025

Abstract

Objective Diabetic nephropathy (DN) is an important complication in diabetic patients that severely impacts their quality of life and life expectancy. Although metabolic and inflammatory responses induced by hyperglycemia are considered the primary pathogenic factors of DN, the specific molecular mechanisms involved remain unclear. Here, we investigated the role of insulin-like growth factor-binding protein 5 (IGFBP5) in DN using in vitro cell experiments and mouse models.

Methods We assessed the effects of high-glucose conditions on IGFBP5 expression in glomerular endothelial cells and evaluated its regulatory effects on glycolysis, NLRP3 inflammasome activation, endothelial–mesenchymal transition (EndoMT), and histone lactylation via the suppression of IGFBP5. Furthermore, we evaluated the effects of IGFBP5 on renal fibrosis and confirmed its regulatory mechanisms in DN model mice.

Results Knockdown of IGFBP5 inhibited high glucose-induced EndoMT in glomerular endothelial cells, which could also be suppressed by the NLRP3 inflammasome inhibitor MCC950. In addition, silencing of IGFBP5 decreased glycolytic activity and histone lactylation, thereby inhibiting the activation of the NLRP3 inflammasome and EndoMT. Furthermore, in mouse models of DN, IGFBP5 knockdown alleviated renal fibrosis and reduced glycolysis, histone lactylation, NLRP3 inflammasome activation and EndoMT.

Conclusions IGFBP5 promotes NLRP3 inflammasome-induced EndoMT and renal fibrosis by regulating glycolysis-mediated histone lactylation, accelerating the progression of DN. These findings provide a new potential therapeutic target for DN.

Keywords Diabetic kidney disease · H3K18 la · 2-DG · GEnCs · Mesenchymal phenotype

Highlights

- IGFBP5 upregulation under high glucose conditions promotes glycolysis and lactate production, leading to increased histone lactylation (H3K18 la) in glomerular endothelial cells.
- Silencing of IGFBP5 strongly diminishes endothelial–mesenchymal transition (EndoMT) and NLRP3 inflammasome activation triggered by high glucose in both cultured cells and mouse models.
- IGFBP5 knockdown in diabetic nephropathy (DN) mice decreases urinary protein levels, alleviates glomerular damage, and reduces renal fibrosis.

✉ Shaxi Ouyang
 shaxiyouyang@163.com

¹ Hunan Normal University Health Science Center, Changsha 410013, Hunan, People's Republic of China

² Department of Nephrology, Zhuzhou Central Hospital, Zhuzhou 412007, People's Republic of China

³ Department of Nephrology, Hunan Provincial People's Hospital, The First Affiliated Hospital of Hunan Normal University, No. 61 Jie-Fang West Road, Fu-Rong District, Changsha 410005, Hunan, People's Republic of China

Abbreviations

α-SMA	α-Smooth muscle actin
ChIP	Chromatin immunoprecipitation
DN	Diabetic nephropathy
EndoMT	Endothelial-mesenchymal transition
FBS	Fetal bovine serum
FSP-1	Fibroblast-specific protein 1
GAPDH	Glyceraldehyde-3-phosphate dehydrogenase
GEnCs	Glomerular endothelial cells
HE	Hematoxylin and eosin
H3K18 la	Histone H3 lysine 18 lactylation
IGFBP5	Insulin-like growth factor-binding protein 5
IHC	Immunohistochemistry
IL-1β	Interleukin-1β
LDH	Lactate dehydrogenase

LDHA	Lactate dehydrogenase A
NLRP3	Nucleotide-binding oligomerization domain (NOD)
leucine-rich repeat (LRR)	And pyrin domain-containing protein 3
PKM2	Pyruvate kinase M2
qPCR	Quantitative real-time polymerase chain reaction
STZ	Streptozotocin
VE-cadherin	Vascular endothelial-cadherin

Introduction

Diabetes mellitus, a globally prevalent chronic metabolic disease, substantially impacts the quality of life and life expectancy of millions of people [1]. In addition to the direct health issues caused by diabetes, its complications, particularly diabetic nephropathy (DN), exacerbate the complexity and severity of the disease. DN is the most common renal complication in diabetic patients and a major cause of end-stage renal disease [2, 3]. Substantial advancements have been made in deciphering the pathogenesis of DN over the last several decades. Numerous studies have indicated that chronic hyperglycemia-induced metabolic and inflammatory responses are major contributors to fibrosis in DN [4, 5]. However, the specific molecular mechanisms remain largely unclear.

The insulin-like growth factor (IGF)-binding protein (IGFBP) family, which consists of seven members, plays crucial roles in kidney diseases, particularly DN [6]. Among these genes, IGFBP1, IGFBP3, IGFBP4, and IGFBP5 are closely associated with diabetes and DN [6]. IGFBP1, IGFBP3, and IGFBP4 contribute to kidney fibrosis and glomerular dysfunction through the modulation of IGF signaling [7, 8]. However, IGFBP5 has attracted increased attention because of its overexpression in fibrotic tissues and its involvement in dysregulated glycolysis in DN [9].

IGFBP5, unlike other members of the IGFBP family, has garnered increasing attention due to its involvement in the fibrotic tissues and the dysregulation of glycolysis in DN. This highlights its unique role in the disease, extending beyond the modulation of IGF signaling. Recently, increasing attention has been given to the role of IGFBP5 in diabetes and its complications, including DN [9–11]. IGFBP5 is a multifunctional protein that regulates the function of IGF by binding to it [12]. IGFBP5 is overexpressed in fibrotic tissues and contributes to the progression of fibrosis [13, 14]. In the context of DN, IGFBP5 has been implicated in the dysregulation of glycolysis, where hyperglycemia alters this central metabolic pathway, leading to increased lactate production [9]. Elevated lactate levels contribute to histone lactylation, particularly histone H3 lysine 18 lactylation (H3K18la), which is a key modification involved in the regulation of gene expression [15, 16]. This histone modification

has been linked to the activation of the NLRP3 inflammasome, a critical mediator of inflammation [17, 18]. The activation of NLRP3 can drive the fibrotic response and renal histopathological lesions in DN [19]. The inhibition of NLRP3 inflammasome activation can ameliorate renal inflammation and fibrosis [20].

Dysfunction of glomerular endothelial cells (GEnCs) plays a critical role in the development of DN [21]. In recent years, endothelial–mesenchymal transition (EndoMT), defined as a decrease in the endothelial phenotype and an increase in the mesenchymal phenotype, has contributed to the pathogenesis of fibrosis. A hyperglycemic state induces EndoMT in GEnCs and exacerbates renal fibrosis in DN [22]. Additionally, inflammatory signaling factors can induce or promote EndoMT, and blocking inflammatory signals may be a more effective strategy for inhibiting EndoMT and related diseases [23]. Lv et al. reported that activation of the NLRP3 inflammasome is associated with EndoMT-mediated pulmonary fibrosis [24]. Inhibiting the NLRP3 inflammasome may reduce lung inflammation and fibrosis by regulating EndoMT [25].

In summary, in DN, IGFBP5 promotes EndoMT and renal fibrosis by regulating glycolysis-mediated histone lactylation (H3K18la), thereby activating the NLRP3 inflammasome. Our findings reveal the mechanisms of IGFBP5 in kidney pathology and highlight potential therapeutic opportunities for targeting IGFBP5 in the context of DN.

Materials and methods

Cell culture and treatment

Mouse GEnCs from Procell (CP-M063, Wuhan, China) were cultured in DMEM supplemented with 10% FBS (Gibco) and 1% streptomycin–penicillin. Afterward, the cells were treated with 5 mM glucose (control group), 20 mM mannitol, 5 mM glucose (mannitol group), or 25 mM glucose (high-glucose group) for 72 hours [26]. For additional treatments, cells in the high-glucose group were treated with MCC950 (NLRP3 inflammasome inhibitor, 10 μ M; Sigma–Aldrich, USA) to assess the effect of NLRP3 inhibition [27]. The cells in the high-glucose group were treated with 2-deoxy-D-glucose (2-DG, a glycolysis inhibitor; 2 mM, Sigma–Aldrich) to examine the impact of glycolysis inhibition [28].

Cell transfection

Short hairpin RNA (shRNA) against IGFBP5 (sh-IGFBP5) and negative control (sh-NC) plasmids were designed (GenePharma, Shanghai, China) to specifically knock down IGFBP5 expression in GEnCs. For transfection, GEnCs were plated in 6-well plates (2×10^5 cells/well) and incubated overnight until they reached approximately 70–80% confluence. The following

day, transfection was carried out by using Lipofectamine™ 3000 (Thermo Fisher Scientific) according to the manufacturer's instructions. The cells were incubated for 4–6 h, after which the transfection medium was replaced with fresh medium. Transfection efficacy was evaluated 24–48 h later using quantitative real-time PCR (qPCR) and Western blot analysis.

qPCR

Total RNA was isolated with TRIzol reagent (15596026, Thermo Fisher Scientific), and cDNA was synthesized with a cDNA synthesis kit (04897030001, Roche). qPCR was conducted with LightCycler 480 SYBR Green I Master Mix (04887352001, Roche). Each reaction utilized 2 µL of diluted cDNA in 10 µL of SYBR Green Master Mix. The expression of genes was determined using the $2^{-\Delta\Delta C_t}$ method. GAPDH served as the internal control. The primers used are listed in Table 1.

Western blot

GEnCs and kidney tissues were homogenized in RIPA lysis buffer (Beyotime, Shanghai, China), and the lysates were centrifuged at $12,000 \times g$ for 15 min at 4 °C. A BCA protein assay kit (Beyotime) was subsequently used to determine protein concentrations. Approximately 30 µg of lysate was separated via SDS–PAGE and subsequently transferred to PVDF membranes. The membranes were incubated with 5% nonfat dry milk in TBST to block nonspecific binding. Subsequently,

the membranes were incubated with primary antibodies: lactate dehydrogenase A (LDHA; 19987–1-AP, 1:5000, Proteintech, Wuhan, China), pan histone lysine lactylation (Pan-Kla; PTM-1401RM; 1:1000, PTM BIO, Hangzhou, China), H3K18 la (PTM-1406RM, 1:1000, PTM BIO), histone H3 (PTM-6613, 1:2000, PTM BIO), pyruvate kinase M2 (PKM2; 15822–1-AP, 1:5000, Proteintech), CD31 (ab281583, 1:1000, Abcam, USA), VE-cadherin (ab33168, 1:1000, Abcam), α -SMA (ab124964, 1:10,000, Abcam), FSP-1 (ab197896, 1:1000, Abcam), NLRP3 (68102–1-Ig, 1:5000, Proteintech), cleaved caspase 1 (ARG57293, 1:1000, Arigo Biolaboratories, Shanghai, China), IL-1 β (26048–1-AP, 1:2000, Proteintech), IGFBP5 (55205–1-AP, 1:500, Proteintech), and β -actin (20536–1-AP, 1:5000, Proteintech) overnight at 4 °C. The membranes were subsequently incubated with secondary antibodies for 60 min. Finally, the target proteins were detected via an enhanced chemiluminescence (ECL) kit (Beyotime) and quantified by ImageJ software.

Lactate production assay

A Lactate Assay Kit (E-BC-K044-S, Elabscience) was used to determine the amount of lactate. Briefly, 20 µL of the supernatant was mixed with 1 mL of Enzyme Working Solution, Chromogenic Agent, or Stop Solution (provided in the kit). The absorbance was measured at 530 nm to calculate the amount of lactate.

LDH activity assay

An LDH Assay Kit (E-BC-K046-M, Elabscience) was used to determine LDH activity. Briefly, the cells were homogenized in physiological saline and centrifuged at $10,000 \times g$ for 10 min at 4 °C. The supernatant was collected for further analysis. LDH activity was then calculated at 450 nm.

Chromatin immunoprecipitation (ChIP)-qPCR

H3K18 la levels in the promoter regions of the NLRP3 and IL-1 β genes were analyzed using a ChIP-qPCR assay. Briefly, GEnCs were crosslinked with 1% formaldehyde for 10 min at room temperature, quenched with 125 mM glycine for 5 min, and lysed in lysis buffer containing protease inhibitors. Chromatin was sheared into 200–500 bp fragments using sonication. After dilution, the chromatin was incubated overnight at 4 °C with either normal IgG (negative control) or H3K18 la (PTM-1427RM, PTM BIO) antibodies. The immune complexes were captured via protein A/G agarose beads and eluted with a specific buffer. Crosslinking was reversed by heating, and the DNA was purified. qPCR was performed to assess the enrichment of NLRP3 and IL-1 β DNA using the following primers: NLRP3 (forward: 5'-GGA AGA TGT TGA GGA GGA GG-3'; reverse:

Table 1 Sequences of primers for qPCR analysis

Gene	Primer sequence
CD31	Forward: 5'-CCAAAGCCAGTAGCATCATGGTC-3' Reverse: 5'-GGATGGTGAAGTTGGCTACAGG-3'
IL-1 β	Forward: 5'-TGGACCTTCCAGGATGAGGACA-3' Reverse: 5'-GTTTCATCTCGGAGCCTGTAGTG-3'
NLRP3	Forward: 5'-TCACAACCTCGCCAAGGAGGAA-3' Reverse: 5'-AAGAGACCACGGCAGAAGCTAG-3'
VE-cadherin	Forward: 5'-GAACGAGGACAGCAACTTCACC-3' Reverse: 5'-GTTAGCGTGCTGGTTCAGTCA-3'
α -SMA	Forward: 5'-TGCTGACAGAGGCACCACTGAA-3' Reverse: 5'-CAGTTGTACGTCCAGAGGCATAG-3'
FSP-1	Forward: 5'-AGCTCAAGGAGCTACTGACCAG-3' Reverse: 5'-GCTGTCCAAGTTGCTCATCACC-3'
IGFBP5	Forward: 5'-AAGAGCTACGGCGAGCAAACCA-3' Reverse: 5'-GCTCGGAAATGCGAGTGTGCTT-3'
GAPDH	Forward: 5'-CATCACTGCCACCCAGAAGACTG-3' Reverse: 5'-ATGCCAGTGAGCTTCCCGTTCAG-3'

α -SMA: α -smooth muscle actin; IL-1 β : interleukin-1 β ; NLRP3: nucleotide-binding oligomerization domain (NOD), leucine-rich repeat (LRR), and pyrin domain-containing protein 3; VE-cadherin: vascular endothelial-cadherin; FSP-1: fibroblast-specific protein 1; GAPDH: glyceraldehyde-3-phosphate dehydrogenase

5'-GCG GAA GAT GAA GAA AGG AAG-3') and IL-1 β (forward: 5'-GGA TGA GGA CCC AAA GGA GA-3'; reverse: 5'-CCT GGG GTC CAC ACG AC-3'). Enrichment was calculated by comparing the DNA levels of target genes to those of the normal IgG control, reflecting histone modification (H3K18 la) and gene regulation in the context of DN.

Animal models and treatment

Six-week-old male C57BL/6 J mice from Vital River (Beijing, China) were divided into four groups ($n = 6$ per group): control, streptozotocin (STZ), STZ + adeno-associated virus (AAV)-sh-NC, and STZ + AAV-sh-IGFBP5. Diabetes was induced in the STZ groups through five consecutive days of intraperitoneal injections of 50 mg/kg STZ. Diabetes was confirmed after the injections by measuring fasting blood glucose levels, with levels exceeding 16.7 mmol/L classified as diabetic. For knockdown of IGFBP5 in the mouse kidney, AAV2/2 carrying sh-IGFBP5 was injected into the tail vein of the mice at a dose of 1×10^{12} viral genome particles 2 weeks after the first STZ injection. After 12 weeks, 24-h urine samples were collected from all the mice to measure urinary protein. The mice were then sacrificed, and kidney tissues were harvested for histological analysis, including hematoxylin and eosin (HE)/Masson staining and immunohistochemistry, to assess glomerular injury. All animal experimental procedures were approved by the Institutional Ethics Committee.

HE and Masson staining

Kidney samples were fixed in 4% paraformaldehyde for 24 h and then dehydrated and embedded in paraffin. With a rotary microtome, continuous sections of 4 μ m thickness were sliced and mounted on slides for further analysis. The paraffin sections were deparaffinized in xylene, rehydrated through a graded alcohol series, and rinsed with water. HE staining was performed to assess glomerular injury, whereas Masson staining was used to evaluate collagen deposition and interstitial lesions.

Immunohistochemistry (IHC)

After the sections were deparaffinized, rehydrated, and subjected to antigen retrieval, endogenous peroxidase activity was blocked using hydrogen peroxide (3%, 10 min). Next, the tissue sections were incubated with a 5% BSA blocking solution for 1 h to prevent nonspecific binding. Primary antibodies (CD31: ab281583, 1:4000; α -SMA: ab124964, 1:1000; Abcam; IGFBP5: 55205-1-AP, 1:200; Proteintech) were applied and incubated overnight at 4 $^{\circ}$ C. The following day, after washing, the sections were incubated with biotinylated secondary antibodies and a streptavidin-HRP

conjugate. The DAB substrate was used for visualization, producing a brown signal indicating positive staining. The sections were then counterstained with hematoxylin, dehydrated, cleared, and mounted for microscopic analysis.

Immunofluorescence staining

Renal tissue sections were obtained and fixed in 4% paraformaldehyde, followed by paraffin embedding and 5 μ m sectioning. Immunofluorescence staining was performed using primary antibodies against CD31 (Arigo, ARG52748 or ARG56119, 1:50), IGFBP5 (Proteintech, 55205-1-AP, 1:50), and α -SMA (Abcam, ab124964, 1:250; or ab240654, 1:50). After incubation with secondary antibodies conjugated to Alexa Fluor 488 (Thermo Fisher Scientific, A-11034/A-11029) or Alexa Fluor 594 (Thermo Fisher Scientific, A-11037/A-11032), the nuclei were stained with DAPI (Sigma-Aldrich, D9542). Fluorescence images were captured using a confocal microscope (Olympus, FV3000), and colocalization analysis was conducted using ImageJ software.

Statistical analysis

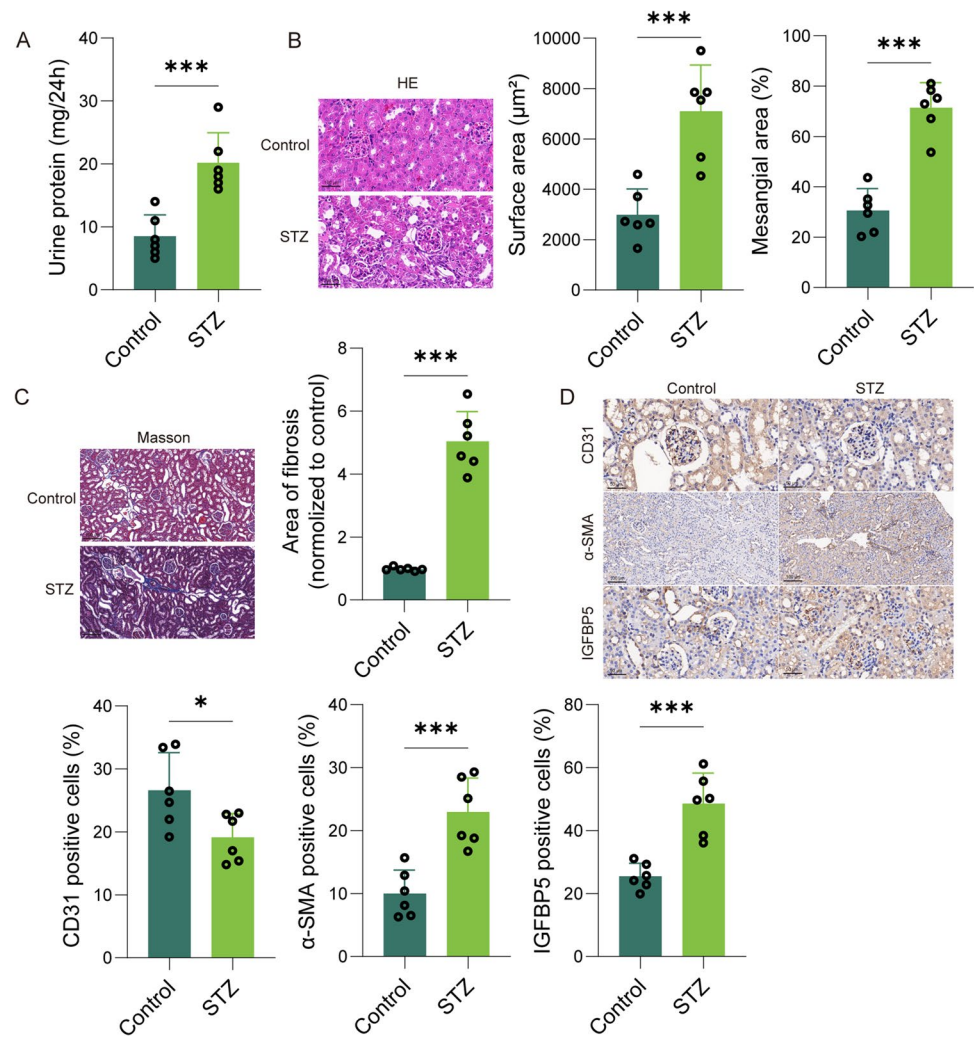
The data are presented as the means \pm standard deviations (SDs). Statistical analyses were conducted using GraphPad Prism 9.0 software (GraphPad Software, Inc.). Comparisons were made using one-way ANOVA followed by Tukey's post hoc test (multiple groups) or two-tailed Student's *t* test (two groups). A *p* value of less than 0.05 was considered statistically significant.

Results

DN progression is accompanied by EndoMT and the upregulation of IGFBP5

To investigate the association between EndoMT and the progression of DN, we established DN mouse models. As shown in Fig. 1A, the STZ-induced mice presented a significant increase in 24-h urinary protein levels. The results of the quantitative HE staining revealed that the glomerular and mesangial areas in the STZ group were significantly increased compared to the control group (Fig. 1B). The quantitative result of Masson staining further revealed substantial collagen deposition and interstitial fibrosis in the kidney tissues of the DN models, in contrast to the minimal fibrosis observed in the control group (Fig. 1C). IHC analysis was used to quantify the expression of specific markers associated with EndoMT. The results revealed significant downregulation of the endothelial marker CD31 and upregulation of the mesenchymal marker α -SMA, along with increased expression of IGFBP5 in the kidney tissues of the

Fig. 1 DN progression is accompanied by EndoMT and the upregulation of IGFBP5. **(A)** Kit assay for 24-h urinary protein. **(B)** Representative images of HE staining and quantitative analysis (glomerular and mesangial surface areas). **(C)** Representative images of Masson's staining and quantitative assessment of fibrosis. **(D)** IHC for CD31, α -SMA, and IGFBP5 expression. $n = 6$. * $p < 0.05$, ** $p < 0.01$, *** $p < 0.001$



DN models, confirming the occurrence of EndoMT during the progression of DN (Fig. 1D). These findings indicate that EndoMT occurs during DN progression, along with elevated IGFBP5 expression in DN.

High glucose induces EndoMT in GEnCs by upregulating IGFBP5

We subsequently developed an in vitro cell evaluation model and found that high glucose conditions downregulated CD31 and VE-cadherin but upregulated α -SMA, FSP-1, and IGFBP5 (Fig. 2A, B). To further explore the role of IGFBP5 in EndoMT, we knocked down IGFBP5 in GEnCs subjected to high-glucose conditions. The knockdown of IGFBP5 notably elevated the mRNA and protein expression of CD31 and VE-cadherin while simultaneously reducing the mRNA and protein levels of α -SMA and FSP-1 (Fig. 2C, D). These findings suggest that silencing IGFBP5 effectively inhibits high glucose-induced EndoMT in GEnCs.

IGFBP5 mediates EndoMT in GEnCs by activating the NLRP3 inflammasome

The activation of the NLRP3 inflammasome can induce EndoMT [24], and we investigated the mechanism by which IGFBP5 mediates EndoMT in GEnCs via the NLRP3 inflammasome. The results revealed that high-glucose conditions led to significant increases in the protein levels of NLRP3, cleaved caspase-1, and IL-1 β , suggesting increased activation of the NLRP3 inflammasome (Fig. 3A). This upregulation was substantially reduced after knockdown of IGFBP5, which indicates that IGFBP5 plays a critical role in facilitating NLRP3 inflammasome activation under high-glucose conditions (Fig. 3A). Furthermore, the inhibition of NLRP3 inflammasome activation led to increased levels of CD31 and VE-cadherin, both at the mRNA and protein levels, coupled with a decrease in the levels of the mesenchymal markers α -SMA and FSP-1 (Fig. 3B, C). This shift in marker expression indicates suppression of the EndoMT process. Collectively, these findings suggest that

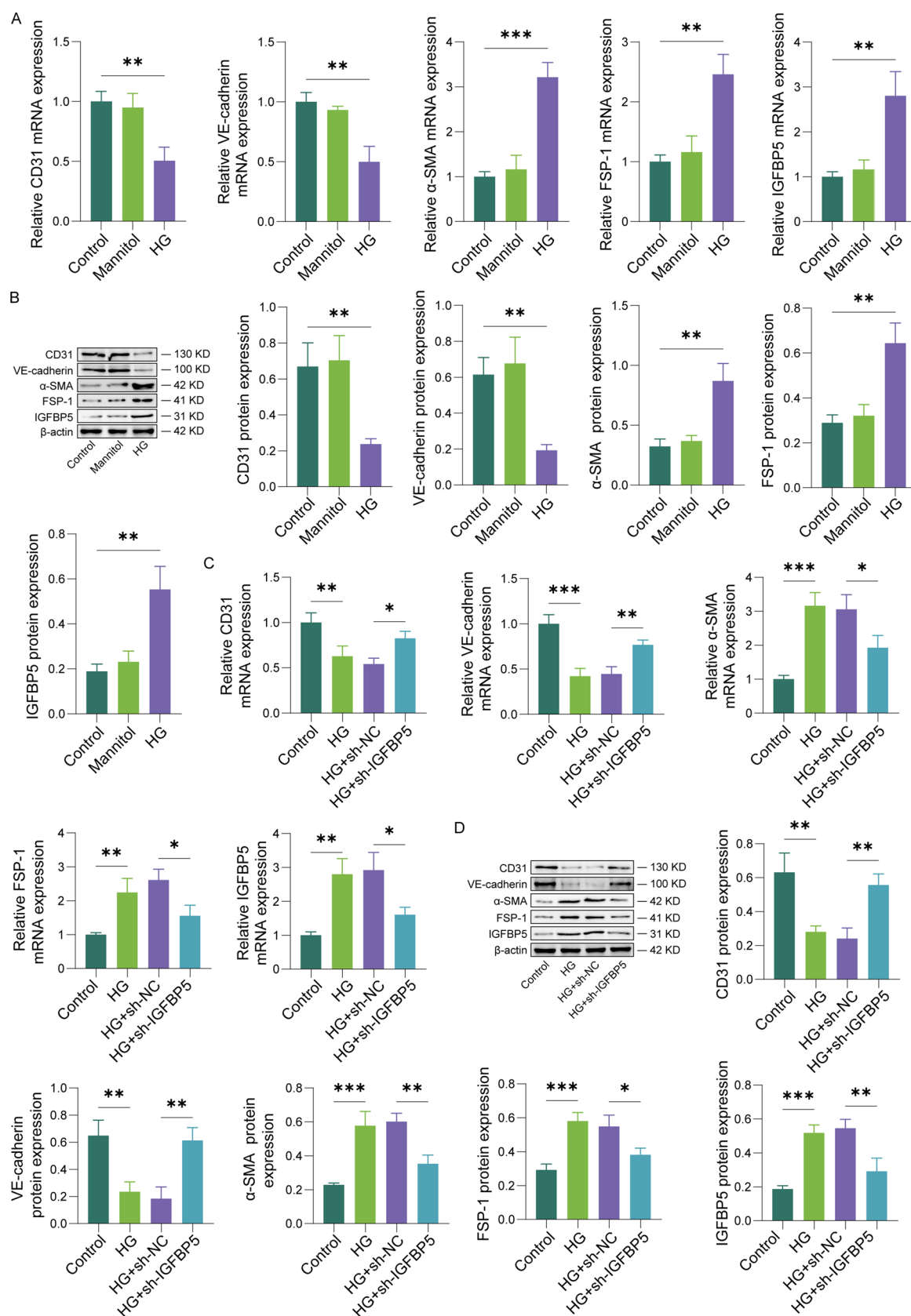


Fig. 2 High glucose induces EndoMT in GEnCs by upregulating IGFBP5. (A–B) qPCR and Western blot analysis of the expression levels of CD31, VE-cadherin, α -SMA, FSP-1, and IGFBP5 in mouse GEnCs. (C–D) qPCR and Western blot analysis of the effects of IGFBP5 on CD31, VE-cadherin, α -SMA, and FSP-1 expression. $n=3$. * $p < 0.05$, ** $p < 0.01$, *** $p < 0.001$. HG, high glucose

IGFBP5 contributes to the induction of EndoMT in GEnCs, primarily through the activation of the NLRP3 inflammasome. IGFBP5 knockdown disrupts the pathway leading to NLRP3 inflammasome activation, which in turn prevents the transition of endothelial cells into a mesenchymal phenotype, thereby inhibiting EndoMT.

IGFBP5 regulates the activation of the NLRP3 inflammasome via glycolysis

To elucidate the mechanism by which IGFBP5 influences NLRP3 inflammasome activation through glycolysis, we conducted a series of experiments to characterize the metabolic and inflammatory responses to high glucose. Our study also revealed that exposure to high glucose led to a significant increase in lactate levels and LDH activity, which are markers of increased glycolytic flux. Notably, these effects were substantially suppressed when IGFBP5 was knocked down, indicating that IGFBP5 plays a critical role in driving glycolysis under hyperglycemic conditions (Fig. 4A, B). Consistent with these findings, we observed that high glucose significantly upregulated the expression of key glycolytic enzymes, LDHA and PKM2, both of which were effectively downregulated following IGFBP5 knockdown (Fig. 4C). These findings suggest that IGFBP5 is a key regulator of glycolytic enzyme expression and that its knockdown disrupts the glycolytic pathway, leading to reduced lactate production. Further investigation revealed that the suppression of glycolysis by treatment with the glycolysis inhibitor 2-DG led to decreased levels of NLRP3, cleaved caspase-1, and IL-1 β , highlighting the connection between glycolytic activity and inflammasome activation (Fig. 4D). Moreover, inhibiting glycolysis led to the restoration of CD31 and VE-cadherin, along with a decrease in α -SMA and FSP-1, further demonstrating the inhibitory effect on the EndoMT process (Fig. 4E, F). These results indicate that IGFBP5 knockdown inhibits NLRP3 inflammasome activation through the glycolytic pathway, thereby suppressing EndoMT in GEnCs.

IGFBP5 regulates histone lactylation-mediated NLRP3 inflammasome activation

To explore how IGFBP5 regulates NLRP3 inflammasome activation further, we found that, compared with the control group, the high glucose group presented significant increases in lactylation and H3K18 la levels. Treatment

with 2-DG or IGFBP5 knockdown reduced high glucose-induced lactylation and H3K18 la levels (Fig. 5A, B). Furthermore, the knockdown of IGFBP5 significantly reduced the gene expression levels of NLRP3 and IL-1 β in GEnCs exposed to high glucose (Fig. 5C). In these high glucose-induced GEnCs, H3K18 la was found to bind to NLRP3 and IL-1 β , and the knockdown of IGFBP5 notably diminished this binding (Fig. 5D). These results revealed that IGFBP5 functions in regulating histone lactylation and the interaction of H3K18 la with NLRP3 and IL-1 β , thereby influencing the activation of the NLRP3 inflammasome and the inflammatory response.

IGFBP5 knockdown inhibits EndoMT-induced renal fibrosis in DN model mice

We further investigated whether the knockdown of IGFBP5 inhibits renal fibrosis and EndoMT in DN model mice. Our findings indicate that IGFBP5 knockdown significantly reduced urinary protein levels (Fig. 6A) in the mice with DN and alleviated glomerular damage as well as interstitial fibrosis, as shown by the quantitative results of HE staining (Fig. 6B, C). At the molecular level, IGFBP5 knockdown led to the upregulation of the endothelial markers CD31 and VE-cadherin, which are typically downregulated during the EndoMT process. Concurrently, there was a sharp decrease in the levels of the mesenchymal markers α -SMA and FSP-1, along with a decrease in IGFBP5 in the mice with DN (Fig. 6D, E). These molecular changes highlight the inhibitory effect of IGFBP5 knockdown on the EndoMT process. The dual fluorescence results of CD31/IGFBP5 and CD31/ α -SMA also revealed that both IGFBP5 and α -SMA were highly expressed in GEnCs (Fig. 6F, G). Overall, these results indicate that IGFBP5 knockdown mitigates EndoMT and renal fibrosis in the mice with DN.

IGFBP5 knockdown inhibits glycolysis-mediated histone lactylation and NLRP3 inflammasome activation in DN

Similarly, at the animal level, we observed that NLRP3 and IL-1 β were upregulated in the kidney tissues of the mice with DN. The knockdown of IGFBP5 significantly downregulated the expression of NLRP3 and IL-1 β (Fig. 7A). We also observed that histone lactylation, as indicated by elevated Pan-K1a and H3K18 la expression, was increased in the kidneys of the mice with DN. Notably, the knockdown of IGFBP5 significantly reduced these histone lactylation levels (Fig. 7B). Additionally, the expression levels of LDHA and PKM2 were elevated in the kidney tissues of the mice with DN, and IGFBP5

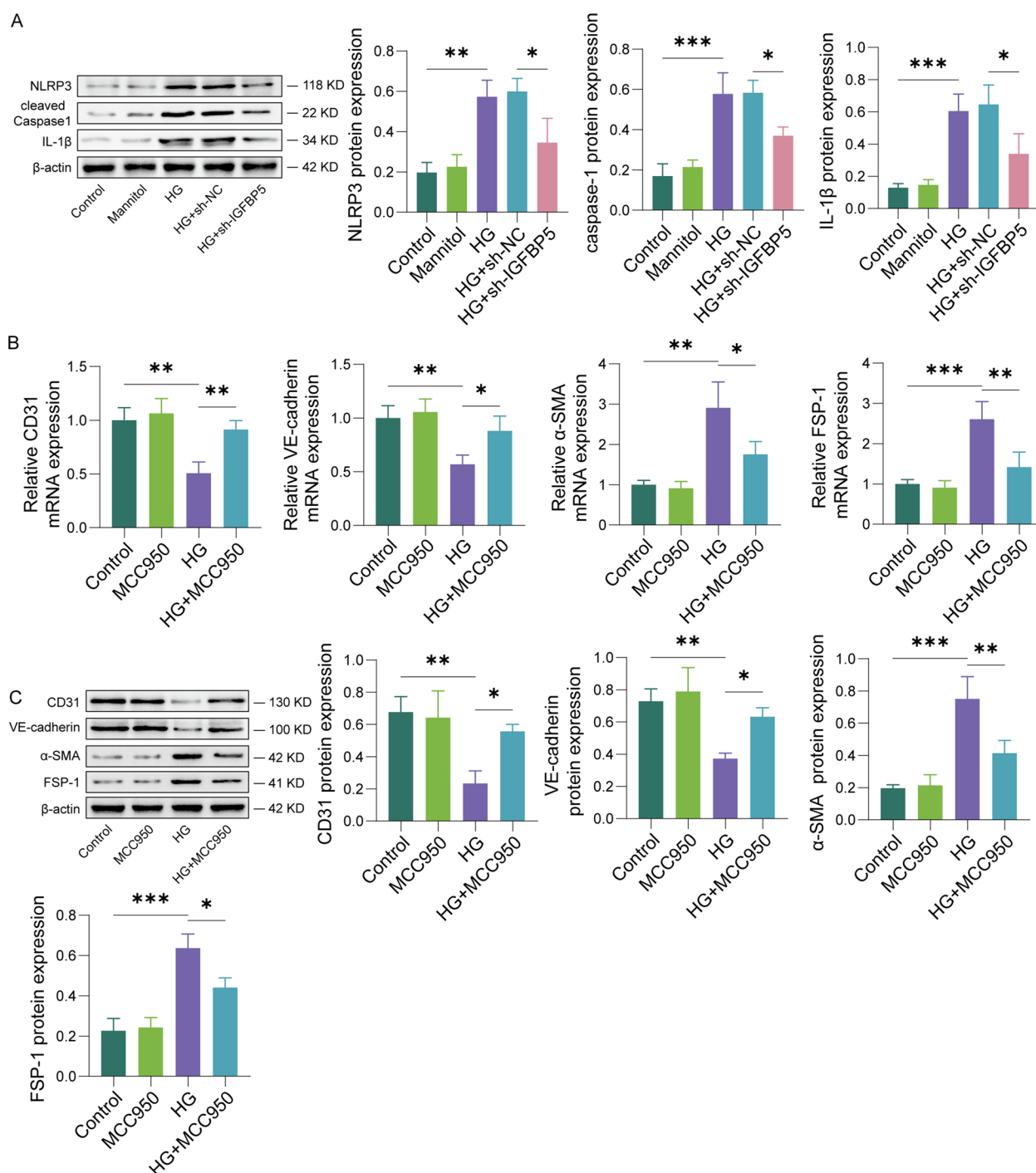


Fig. 3 IGFBP5 mediates EndoMT in GEnCs by activating the NLRP3 inflammasome. **(A)** Western blot analysis of the levels of NLRP3, cleaved caspase-1, and IL-1β. **(B)** qPCR analysis of CD31,

VE-cadherin, α-SMA, and FSP-1 mRNA levels. **(D)** Western blot analysis of CD31, VE-cadherin, α-SMA, and FSP-1 protein levels. $n = 3$. * $p < 0.05$, ** $p < 0.01$, *** $p < 0.001$. HG, high glucose

knockdown markedly decreased LDHA and PKM2 levels (Fig. 7C). These results suggest that IGFBP5 knockdown inhibits glycolysis-mediated histone lactylation and activates the NLRP3 inflammasome.

Discussion

DN is a prevalent complication among diabetic patients, substantially decreasing their quality of life and life expectancy. In this study, we discovered that high-glucose

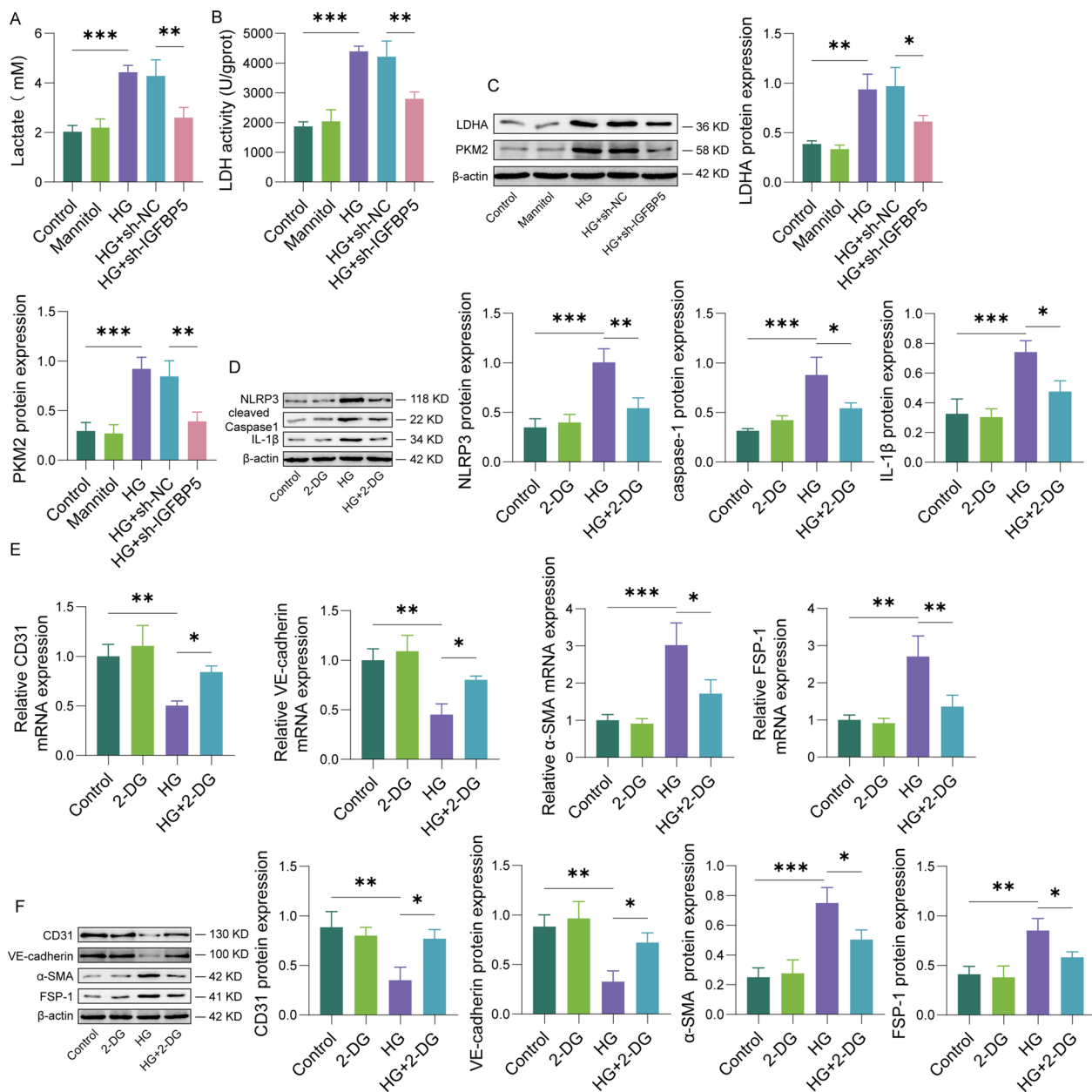


Fig. 4 IGFBP5 regulates the activation of the NLRP3 inflammasome via glycolysis. (**A–B**) Kit assays for lactate production and LDH activity. (**C**) Western blot analysis of LDHA and PKM2 expression. (**D**) Western blot analysis of the levels of NLRP3, cleaved caspase-1, and

IL-1β. (**E–F**) qPCR and Western blot analyses of the CD31, VE-cadherin, α-SMA, and FSP-1 mRNA and protein levels. $n = 3$. $*p < 0.05$, $**p < 0.01$, $***p < 0.001$. HG, high glucose

conditions lead to substantial upregulation of IGFBP5, which, in turn, promotes glycolytic activity and increases lactate production, thereby promoting EndoMT through activation of the NLRP3 inflammasome. By knocking down IGFBP5, we significantly inhibited high glucose-induced glycolysis, NLRP3 inflammasome activation, and EndoMT in GEnCs. Furthermore, in a DN mouse model, IGFBP5 knockdown resulted in lower urinary protein levels, lessened glomerular damage, and a marked reduction

in interstitial fibrosis, highlighting the therapeutic potential of targeting IGFBP5 in DN.

IGFBP5, a conserved member of the IGFBP family, is critically involved in the regulation of various fibrosis-related diseases. IGFBP5 is recognized as a regulator of the fibroblast–myofibroblast transition and plays an important role in cardiac fibrosis [14]. Upregulation of IGFBP5 promotes the transformation of endothelial cells into a fibrous phenotype, resulting in myocardial fibrosis and hypertrophy

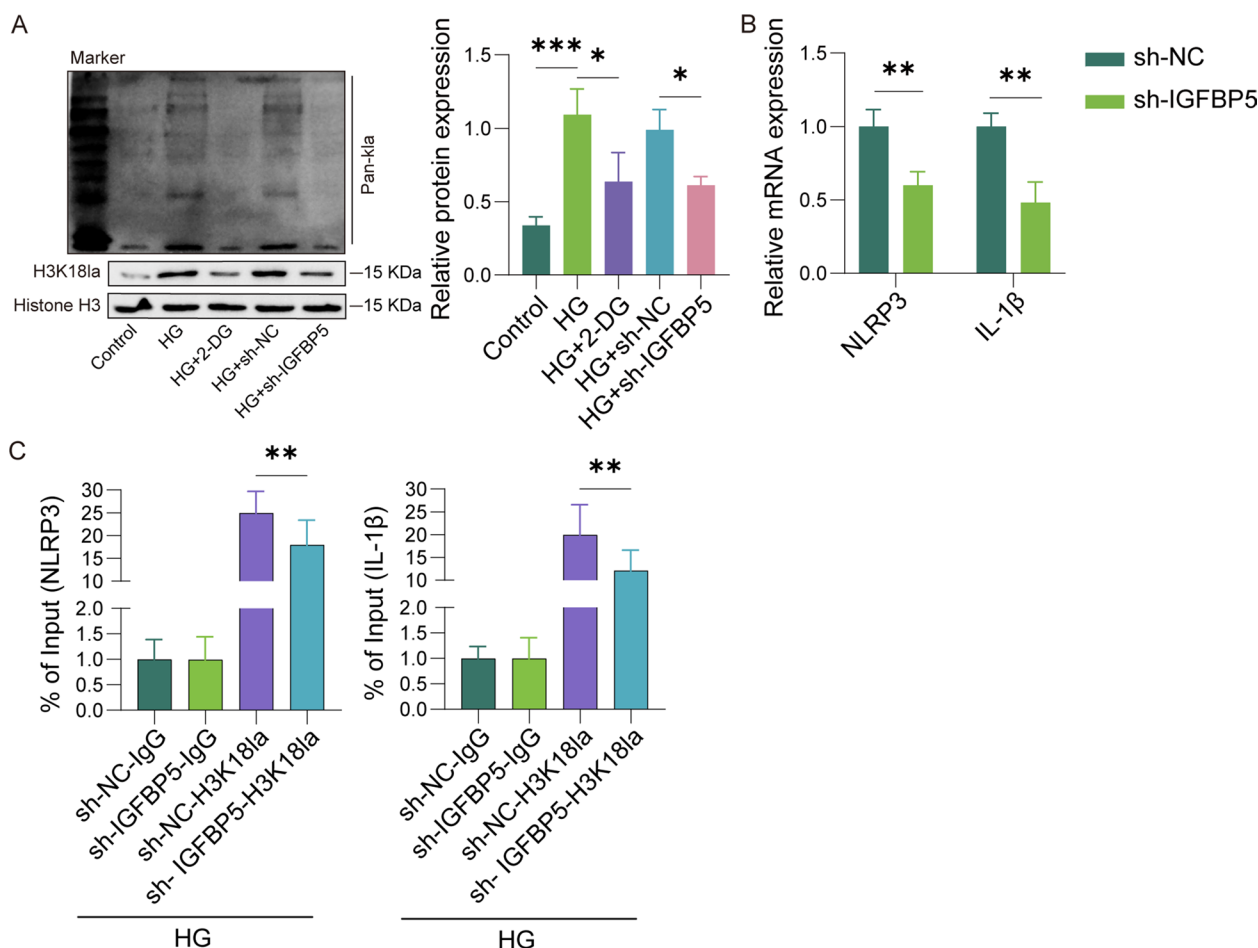


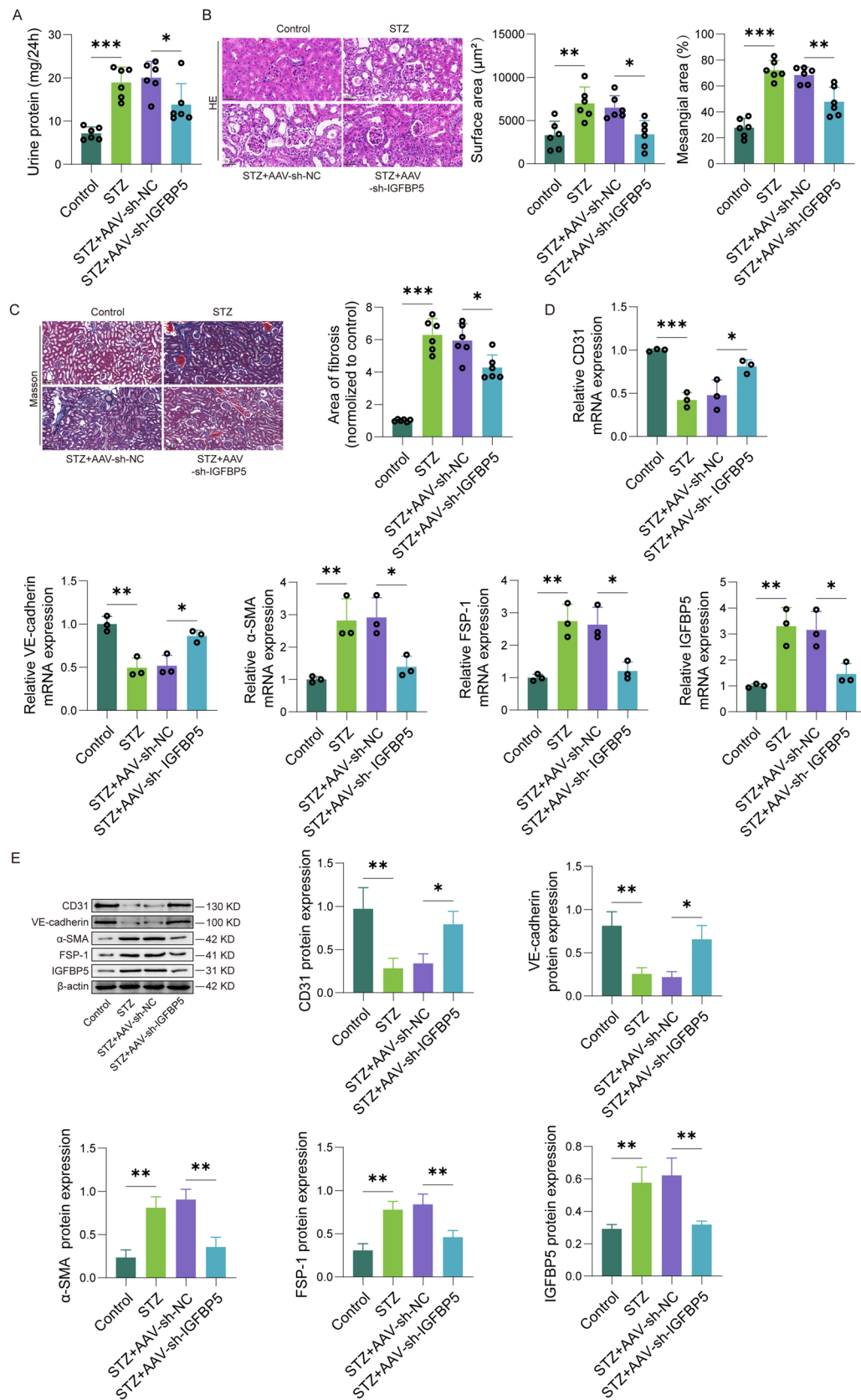
Fig. 5 IGFBP5 regulates histone lactylation-mediated NLRP3 inflammasome activation. **(A)** Western blot analysis of total Pan-Kla (the leftmost blots are markers) and H3K18 la levels. **(B)** qPCR analysis

of NLRP3 and IL-1β expression. **(C)** ChIP-qPCR analysis of H3K18 la modifications on NLRP3 and IL-1β. $n = 3$. * $p < 0.05$, ** $p < 0.01$, *** $p < 0.001$. HG, high glucose

[29]. Consistently, we found that IGFBP5 was increased in high glucose-induced GEnCs and DN model mice. Silencing of IGFBP5 reduced EndoMT and renal fibrosis. In addition, a study reported that the upregulation of IGFBP5 promoted the inflammatory responses of GEnCs by enhancing glycolysis [9]. Lactate is a product of glycolysis that is generated from pyruvate by LDH and plays a crucial role in both physiological and pathological processes. A reduction in lactate produced through glycolysis leads to decreased levels of histone lactylation. Conversely, an increase in aerobic glycolysis can increase lactate production and promote histone lactylation of downstream genes, thereby facilitating the inflammatory responses and contributing to renal fibrosis [30]. In a hyperglycemic state, increased glucose levels lead to the formation of nonenzymatic glycation products, such as advanced glycation end products (AGEs). For example, AGEs promote the inflammatory responses by activating the NF-κB pathway, which in turn affects the expression of cytokines and growth factors, potentially leading to the

upregulation of IGFBP5 [9]. Oxidative stress induced by hyperglycemia is also a key factor in regulating IGFBP5 expression. Hyperglycemia increases the production of reactive oxygen species (ROS), which activate the MAPK and PI3K/Akt signaling pathways, potentially modulating the gene expression of IGFBP5. Studies suggest that oxidative stress can directly or indirectly promote IGFBP5 transcription by affecting transcription factors such as AP-1 and NF-κB [31]. In this study, IGFBP5 was found to increase

Fig. 6 IGFBP5 knockdown inhibits EndoMT-induced renal fibrosis in DN model mice. **(A)** Kit assay for 24-h urinary protein. **(B)** Representative images of HE staining and quantitative analysis (glomerular and mesangial surface areas). **(C)** Representative images of Masson's staining and quantitative assessment of fibrosis. **(D)** qPCR for CD31, VE-cadherin, α-SMA, FSP-1, and IGFBP5 expression. **(E)** Western blot analysis of CD31, VE-cadherin, α-SMA, FSP-1, and IGFBP5 protein levels. **(F, G)** Dual fluorescence results for CD31/IGFBP5 and CD31/α-SMA. $n = 6$. * $p < 0.05$, ** $p < 0.01$, *** $p < 0.001$



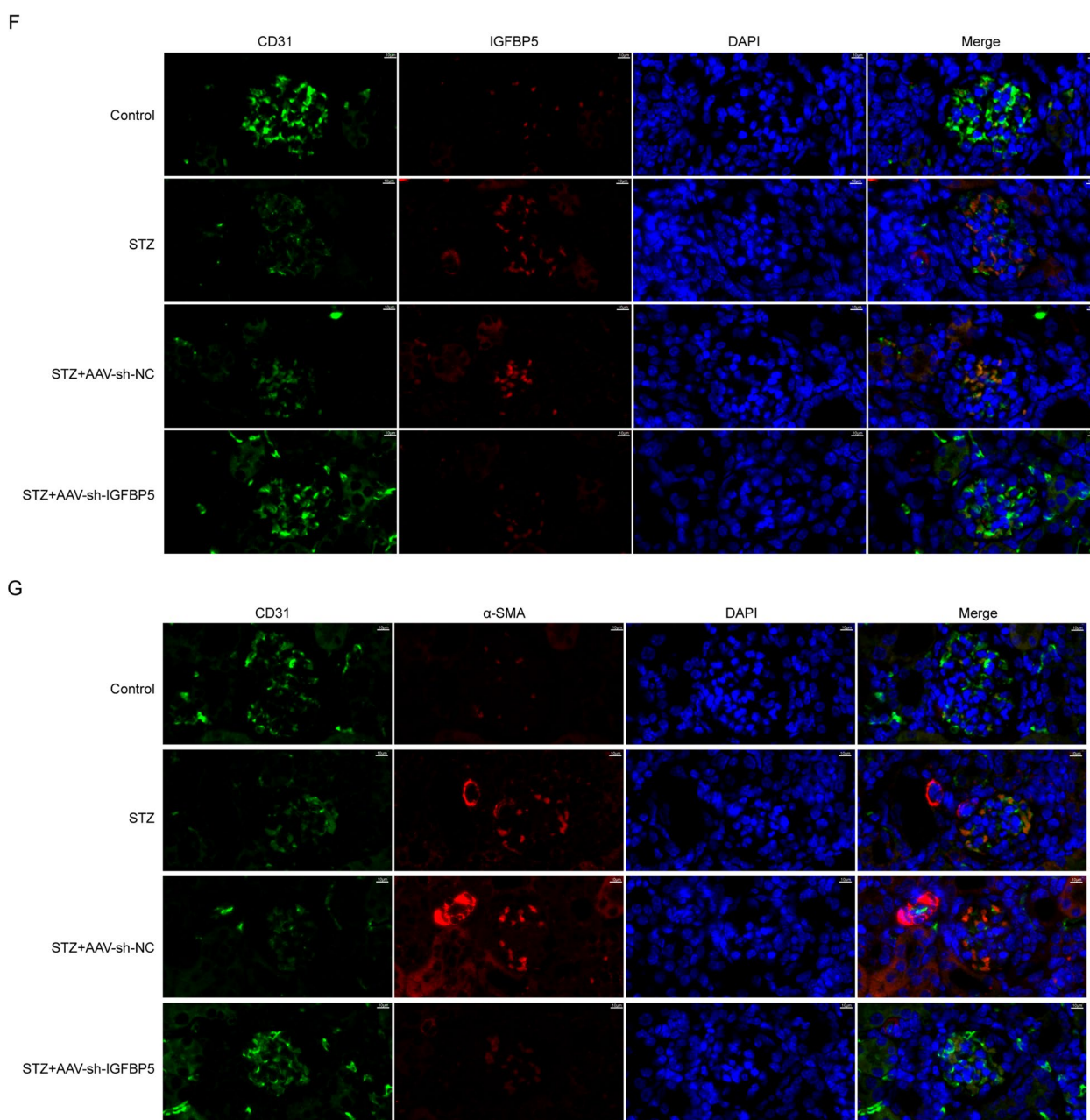


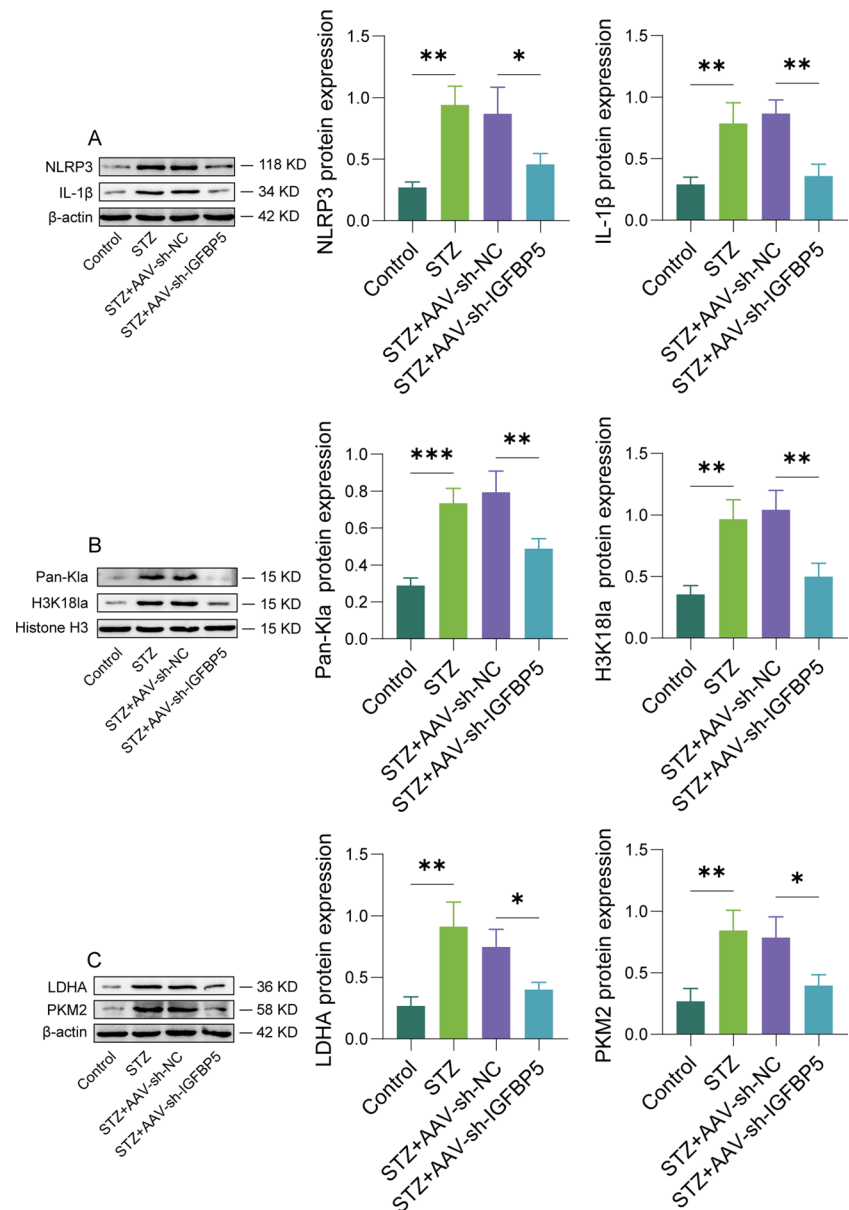
Fig. 6 (continued)

lactate levels, and the accumulation of lactate increased histone H3K18 lactylation levels. This histone lactylation can regulate a series of genes associated with inflammation, including NLRP3 and IL-1 β .

The role of the NLRP3 inflammasome in DN has been well documented, with its activation closely linked to renal fibrosis and inflammatory responses [20]. Under high-glucose conditions, endothelial cells lose their specific phenotype and transform into cells with mesenchymal

characteristics, a process known as EndoMT. This transformation is considered a crucial mechanism for renal fibrosis in DN [32]. Our results showed that IGFBP5 knockdown significantly inhibited EndoMT and reduced NLRP3 inflammasome activation both in vitro and in vivo. The role of the NLRP3 inflammasome in DN has been extensively studied. For example, NLRP3 inflammasome activation is closely associated with renal fibrosis and inflammatory responses in DN [33]. The NLRP3 inflammasome, a multiprotein

Fig. 7 IGFBP5 knockdown inhibits glycolysis-mediated histone lactylation and NLRP3 inflammasome activation in DN. **(A)** Western blot analysis of the NLRP3 and IL-1 β levels. **(B)** Western blot analysis of Pan-Kla and H3K18 la levels. **(C)** Western blot analysis of LDHA and PKM2 levels. n = 6. * p < 0.05, ** p < 0.01, *** p < 0.001



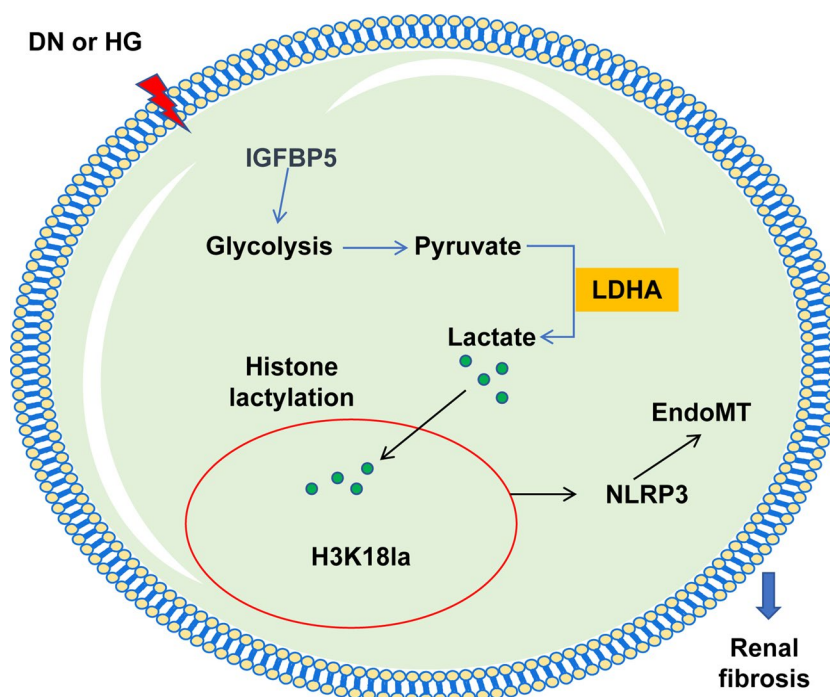
complex, responds to intracellular danger signals (such as metabolic disturbances and pathogen infections)[34], triggering inflammatory responses [25]. Interestingly, while previous studies have highlighted the importance of NLRP3 in DN [35], our research suggests that IGFBP5 may exert its effects on EndoMT largely through the NLRP3 inflammasome pathway, providing new insight into the role of IGFBP5 in DN.

IGFBP2 and IGFBP4 are both upregulated in DN, where they promote inflammation and podocyte apoptosis through mechanisms such as complement activation and oxidative stress [36, 37]. Elevated levels of these proteins exacerbate renal injury and glomerular hypertrophy, making them

potential targets for therapeutic intervention in DN. In contrast, IGFBP6, which is reduced in atherosclerotic conditions, acts protectively by attenuating endothelial inflammation and atherosclerosis through the MVP-c-Jun N-terminal kinase/NF- κ B pathway [38].

In clinical research on DN, urinary protein levels serve as crucial indicators for evaluating renal function impairment [24]. This study revealed a significant reduction in urinary protein levels following the knockdown of IGFBP5, further supporting its potential role in protecting renal function. Additionally, glomerular damage and interstitial fibrosis are the primary pathological features associated with the progression of DN [39]. These injuries not only compromise

Fig. 8 Proposed model depicting the use of IGFBP5 as a glycolysis promoter to induce lactate production and histone lactylation (H3K18la), which activates the NLRP3 inflammasome and subsequent EndoMT, consequently accelerating the renal fibrosis process in DN



the structure and function of the glomerulus but also may trigger local inflammation and fibrotic responses, thereby accelerating the deterioration of renal function [40].

Despite highlighting the important role of IGFBP5 in DN and its potential mechanisms, this study has several limitations. This study relies primarily on in vitro and mouse models and lacks clinical validation with human samples. Additionally, it focuses mainly on glycolysis and histone lactylation, without exploring other potential regulatory pathways or interactions involving IGFBP5. Further research is necessary to confirm these findings in humans and to explore additional mechanisms that may contribute to the progression of DN. Some studies have also indicated that androgens may influence DN progression by modulating immune responses, inflammation, and lipid metabolism [41]. Therefore, the exclusive use of male mice in this study may not adequately represent the effects of gender differences on the progression of DN, which requires further investigation in future research.

Conclusions

This study elucidated the mechanism by which IGFBP5 promoted EndoMT and renal fibrosis by activating the NLRP3 inflammasome through glycolysis-mediated histone lactylation (Fig. 8). The knockdown of IGFBP5 inhibited glycolysis, histone lactylation, and the binding of H3K18la to NLRP3 and IL-1 β , thereby affecting the activation of

the NLRP3 inflammasome. Furthermore, the deletion of IGFBP5 suppressed EndoMT by attenuating NLRP3 inflammasome activation, thereby mitigating the pathological progression of DN. These findings offer new potential therapeutic targets and strategies for the treatment of DN. However, further research is necessary to validate these findings and explore additional mechanisms by which IGFBP5 may influence DN.

Supplementary Information The online version contains supplementary material available at <https://doi.org/10.1007/s00018-025-05718-5>.

Author contributions Shaxi Ouyang guaranteed the integrity of the entire study. Xiaofang Hu and Shaxi Ouyang designed the study and literature research and defined the intellectual content. Wei Chen, Mengwei Li, and Xiangyi Li performed the experiments. Wei Chen and Mengwei Li collected the data. Ming Yang analyzed the data. Xiaofang Hu wrote the main manuscript and prepared the figures. All the authors reviewed the manuscript. These authors contributed equally to this work.

Funding This work was supported by the Natural Science Foundation of Hunan Province (2024JJ9280).

Data availability The datasets used or analyzed during the current study are available from the corresponding author upon reasonable request.

Declarations

Ethics approval and consent to participate All animal experimental procedures were approved by the Institutional Ethics Committee.

Consent for publication Not applicable.

Code availability Not applicable.

Conflict of interest The authors declare that they have no known competing financial interests or personal relationships that could have appeared to influence the work reported in this paper.

Declaration of generative AI and AI-assisted technologies in the writing process During the preparation of this work, the authors did not use any AI-assisted technology.

Open Access This article is licensed under a Creative Commons Attribution-NonCommercial-NoDerivatives 4.0 International License, which permits any non-commercial use, sharing, distribution and reproduction in any medium or format, as long as you give appropriate credit to the original author(s) and the source, provide a link to the Creative Commons licence, and indicate if you modified the licensed material. You do not have permission under this licence to share adapted material derived from this article or parts of it. The images or other third party material in this article are included in the article's Creative Commons licence, unless indicated otherwise in a credit line to the material. If material is not included in the article's Creative Commons licence and your intended use is not permitted by statutory regulation or exceeds the permitted use, you will need to obtain permission directly from the copyright holder. To view a copy of this licence, visit <http://creativecommons.org/licenses/by-nc-nd/4.0/>.

References

- Sun J, Hu W, Ye S, Deng D, Chen M (2023) The Description and Prediction of Incidence, Prevalence, Mortality, Disability-Adjusted Life Years Cases, and Corresponding Age-Standardized Rates for Global Diabetes. *J Epidemiol Glob Health* 13:566–576. <https://doi.org/10.1007/s44197-023-00138-9>
- Narres M et al (2016) The Incidence of End-Stage Renal Disease in the Diabetic (Compared to the Non-Diabetic) Population: A Systematic Review. *PLoS ONE* 11:e0147329. <https://doi.org/10.1371/journal.pone.0147329>
- Chen Y, Lee K, Ni Z, He JC (2020) Diabetic Kidney Disease: Challenges, Advances, and Opportunities. *Kidney Dis (Basel)* 6:215–225. <https://doi.org/10.1159/000506634>
- Srivastava SP et al (2018) SIRT3 deficiency leads to induction of abnormal glycolysis in diabetic kidney with fibrosis. *Cell Death Dis* 9:997. <https://doi.org/10.1038/s41419-018-1057-0>
- Xiang E et al (2020) Human umbilical cord-derived mesenchymal stem cells prevent the progression of early diabetic nephropathy through inhibiting inflammation and fibrosis. *Stem Cell Res Ther* 11:336. <https://doi.org/10.1186/s13287-020-01852-y>
- Wang S, Chi K, Wu D, Hong Q (2021) Insulin-Like Growth Factor Binding Proteins in Kidney Disease. *Front Pharmacol* 12:807119. <https://doi.org/10.3389/fphar.2021.807119>
- AlMajed HT et al (2023) Increased Levels of Circulating IGFBP4 and ANGPTL8 with a Prospective Role in Diabetic Nephropathy. *Int J Molecul Sci* 24:14244. <https://doi.org/10.3390/ijms241814244>
- Yamada PM et al (2010) Evidence of a role for insulin-like growth factor binding protein (IGFBP)-3 in metabolic regulation. *Endocrinology* 151:5741–5750. <https://doi.org/10.1210/en.2010-0672>
- Song C et al (2022) IGFBP5 promotes diabetic kidney disease progression by enhancing PFKFB3-mediated endothelial glycolysis. *Cell Death Dis* 13:340. <https://doi.org/10.1038/s41419-022-04803-y>
- Ji Y, Zhang W, Yang J, Li C (2020) MiR-193b inhibits autophagy and apoptosis by targeting IGFBP5 in high glucose-induced trophoblasts. *Placenta* 101:185–193. <https://doi.org/10.1016/j.placenta.2020.09.015>
- Ock J et al (2023) IGFBP5 antisense and short hairpin RNA (shRNA) constructs improve erectile function by inducing cavernosum angiogenesis in diabetic mice. *Andrology* 11:358–371. <https://doi.org/10.1111/andr.13234>
- Akkiprik M et al (2008) Multifunctional roles of insulin-like growth factor binding protein 5 in breast cancer. *Breast Cancer Res* 10:212. <https://doi.org/10.1186/bcr2116>
- Nguyen XX, Renaud L, Feghali-Bostwick C (2021) Identification of Impacted Pathways and Transcriptomic Markers as Potential Mediators of Pulmonary Fibrosis in Transgenic Mice Expressing Human IGFBP5. *Int J Mol Sci* 22. <https://doi.org/10.3390/ijms22212609>
- Zhao Q et al (2024) The insulin-like growth factor binding protein-microfibrillar associated protein-sterol regulatory element binding protein axis regulates fibroblast-myofibroblast transition and cardiac fibrosis. *Br J Pharmacol* 181:2492–2508. <https://doi.org/10.1111/bph.16314>
- Li F et al (2024) Positive feedback regulation between glycolysis and histone lactylation drives oncogenesis in pancreatic ductal adenocarcinoma. *Mol Cancer* 23:90. <https://doi.org/10.1186/s12943-024-02008-9>
- Lin X et al (2024) Augmentation of scleral glycolysis promotes myopia through histone lactylation. *Cell Metab* 36:511–525.e517. <https://doi.org/10.1016/j.cmet.2023.12.023>
- Hu S et al (2024) Salvianolic Acid B Alleviates Liver Injury by Regulating Lactate-Mediated Histone Lactylation in Macrophages. *Molecules* 29. <https://doi.org/10.3390/molecules29010236>
- Sun S et al (2021) Lactic Acid-Producing Probiotic *Saccharomyces cerevisiae* Attenuates Ulcerative Colitis via Suppressing Macrophage Pyroptosis and Modulating Gut Microbiota. *Front Immunol* 12:777665. <https://doi.org/10.3389/fimmu.2021.777665>
- Ding T et al (2018) Kidney protection effects of dihydroquercetin on diabetic nephropathy through suppressing ROS and NLRP3 inflammasome. *Phytomedicine* 41:45–53. <https://doi.org/10.1016/j.phymed.2018.01.026>
- Wu M et al (2018) NLRP3 deficiency ameliorates renal inflammation and fibrosis in diabetic mice. *Mol Cell Endocrinol* 478:115–125. <https://doi.org/10.1016/j.mce.2018.08.002>
- Fu J, Lee K, Chuang PY, Liu Z, He JC (2015) Glomerular endothelial cell injury and cross talk in diabetic kidney disease. *Am J Physiol Renal Physiol* 308:F287–297. <https://doi.org/10.1152/ajprenal.00533.2014>
- Chen Y, Zou H, Lu H, Xiang H, Chen S (2022) Research progress of endothelial-mesenchymal transition in diabetic kidney disease. *J Cell Mol Med* 26:3313–3322. <https://doi.org/10.1111/jcmm.17356>
- Yoshimatsu Y, Watabe T (2022) Emerging roles of inflammation-mediated endothelial-mesenchymal transition in health and disease. *Inflamm Regen* 42:9. <https://doi.org/10.1186/s41232-021-00186-3>
- Lv Z et al (2018) NLRP3 Inflammasome Activation Contributes to Mechanical Stretch-Induced Endothelial-Mesenchymal Transition and Pulmonary Fibrosis. *Crit Care Med* 46:e49–e58. <https://doi.org/10.1097/ccm.0000000000002799>
- Chen WC, Yu WK, Su VY, Hsu HS, Yang KY (2023) NLRP3 Inflammasome Activates Endothelial-to-Mesenchymal Transition via Focal Adhesion Kinase Pathway in Bleomycin-Induced Pulmonary Fibrosis. *Int J Mol Sci* 24. <https://doi.org/10.3390/ijms242115813>

26. Li X et al (2022) The SETD8/ELK1/bach1 complex regulates hyperglycaemia-mediated EndMT in diabetic nephropathy. *J Transl Med* 20:147. <https://doi.org/10.1186/s12967-022-03352-4>
27. Wu M et al (2021) Inhibition of NLRP3 inflammasome ameliorates podocyte damage by suppressing lipid accumulation in diabetic nephropathy. *Metabolism* 118:154748. <https://doi.org/10.1016/j.metabol.2021.154748>
28. Dong M et al (2024) ASF1A-dependent P300-mediated histone H3 lysine 18 lactylation promotes atherosclerosis by regulating EndMT. *Acta Pharm Sin B* 14:3027–3048. <https://doi.org/10.1016/j.apsb.2024.03.008>
29. Li Y et al (2024) Crosstalk between endothelial cells with a non-canonical EndoMT phenotype and cardiomyocytes/fibroblasts via IGFBP5 aggravates TAC-induced cardiac dysfunction. *Eur J Pharmacol* 966:176378. <https://doi.org/10.1016/j.ejphar.2024.176378>
30. Wang Y et al (2024) The glycolytic enzyme PFKFB3 drives kidney fibrosis through promoting histone lactylation-mediated NF- κ B family activation. *Kidney Int* 106:226–240. <https://doi.org/10.1016/j.kint.2024.04.016>
31. Clemmons DR (2018) Role of IGF-binding proteins in regulating IGF responses to changes in metabolism. *J Mol Endocrinol* 61:T139–t169. <https://doi.org/10.1530/jme-18-0016>
32. Yao W et al (2024) AR/RKIP pathway mediates the inhibitory effects of icariin on renal fibrosis and endothelial-to-mesenchymal transition in type 2 diabetic nephropathy. *J Ethnopharmacol* 320:117414. <https://doi.org/10.1016/j.jep.2023.117414>
33. Wang Y, Sui Z, Wang M, Liu P (2023) Natural products in attenuating renal inflammation via inhibiting the NLRP3 inflammasome in diabetic kidney disease. *Front Immunol* 14:1196016. <https://doi.org/10.3389/fimmu.2023.1196016>
34. Williams BM, Cliff CL, Lee K, Squires PE, Hills CE (2022) The Role of the NLRP3 Inflammasome in Mediating Glomerular and Tubular Injury in Diabetic Nephropathy. *Front Physiol* 13:907504. <https://doi.org/10.3389/fphys.2022.907504>
35. Chen Y et al (2023) The NLRP3 inflammasome: contributions to inflammation-related diseases. *Cell Mol Biol Lett* 28:51. <https://doi.org/10.1186/s11658-023-00462-9>
36. Liang J et al (2025) IGFBP2 and IGFBP4 interact to activate complement pathway in diabetic kidney disease. *Ren Fail* 47:2440528. <https://doi.org/10.1080/0886022x.2024.2440528>
37. Wang X et al (2024) IGFBP2 induces podocyte apoptosis promoted by mitochondrial damage via integrin α 5/FAK in diabetic kidney disease. *Apoptosis* 29:1109–1125. <https://doi.org/10.1007/s10495-024-01974-1>
38. Su M et al (2025) Endothelial IGFBP6 suppresses vascular inflammation and atherosclerosis. *Nat Cardiovasc Res* 4:145–162. <https://doi.org/10.1038/s44161-024-00591-0>
39. Xue R et al (2023) The Molecular Mechanism of Renal Tubulointerstitial Inflammation Promoting Diabetic Nephropathy. *Int J Nephrol Renovasc Dis* 16:241–252. <https://doi.org/10.2147/ijnrd.S436791>
40. Huang R, Fu P, Ma L (2023) Kidney fibrosis: from mechanisms to therapeutic medicines. *Signal Transduct Target Ther* 8:129. <https://doi.org/10.1038/s41392-023-01379-7>
41. Yin L, Qi S, Zhu Z (2023) Advances in mitochondria-centered mechanism behind the roles of androgens and androgen receptor in the regulation of glucose and lipid metabolism. *Front Endocrinol (Lausanne)*. 14:1267170. <https://doi.org/10.3389/fendo.2023.1267170>

Publisher's Note Springer Nature remains neutral with regard to jurisdictional claims in published maps and institutional affiliations.